Quality criteria for control of epidemic process

S. E. Miheev[1], *V. S. Mikheev*[2]

[1] St Petersburg State University, 7–9, Universitetskaya nab., St Petersburg,
  199034, Russian Federation
[2] Kansas State University, 1228, av. Martin Luther King, Manhattan,
  KS 66506, USA

The total number of those infected at the end of an epidemic and the maximum number of infected during an epidemic are considered as two quality criteria for control by delayed isolation of the SIR- and SIRS-type infections. The temporal Barabasi — Albert graph is used to model the contacts between individuals. Simulations are run to estimate optimal delays.

Keywords: delayed isolation, SIR, SIRS, control of epidemics, temporal Barabasi — Albert graph, total number of infected, maximum number of infected, temporal network.

1. Introduction. How can we control the epidemics of type Susceptible → Infected → Recovered (SIR) or Susceptible → Infected → Recovered → Susceptible (SIRS)?

In March 2020, many nations around the world reacted to the spread of COVID-19 through policies of social isolation to help to stop the pandemic and minimize the damage. Isolation typically involves voluntary and non-voluntary restrictions on social interactions. Simply speaking, in-person contacts are limited to the closest circles. Notice that in papers published before 2020, "isolation" usually applied only to the infected individuals. These measures have obvious economic repercussions. So, isolation has its own price. This economic criterion will certainly be studied extensively in the future. In this work, however, we analyze the effect of the isolation on the spread of the disease.

There have already been some examples of this kind of study.

Brownian Motion. One good animation of the Brownian motion approach can be found in [1] and the theoretical support can found in [2].

Differential Equations. The classic differential equations approach is explained well in [3]. The problem of epidemic control using "prevention" (similar to the notion "isolation" in this paper) in percolation model with SIR differential equations considered in [4–7].

The model SIR on differential equations is very popular and as a result many researchers associate the name SIR with it. Nevertheless, here by SIR and SIRS we understand no more than just the concept of transitioning between the states S, I, R.

Both Brownian motion and differential equations are ongoing directions in research. However, they don't fit well to simulate the isolation of all population. So, we will focus on other models.

Contact Networks. We apply the network (graph) approach. The agent-based approach for SIS (Susceptible → Infected → Susceptible) and SIR diseases was developed in [8, 9].

So far we don't see papers considering isolation of all population as method to control the epidemic on a network. However, there are some good works on a problem of epidemic control with isolation of infected people. In [10], authors consider SIS on Erdos — Reni and Barabasi — Albert graphs. Isolation of infected on multilayer network with SIR is considered in [11]. SIS model (no immunity after illness) and multilayer network aren't applicable to COVID-19 and influenza.

We consider SIR and SIRS process on a temporal graph. This graph is built according to Barabasi — Albert preferential attachment mechanism [12], which is known to be one of the best to reflect social connections. Then we modify it by making the edges temporal, meaning they available only at a specific times. The theory of temporal graphs can be found in [13]. Then we run this SIR simulation with 2, 3 and 4 week restriction on communication with "popular" nodes (ones with the degree equal or greater than 5), starting with different delays from the beginning of the epidemic process. The result is presented as plots of the difference of infected and recovered. The Section 5, repeats the experiment for SIRS model. The Python computer code can be found in an open access at [14].

Disclaimer. Of course, our work is inspired by unprecedented event of COVID-19 outbreak. However, this paper should not be seen as a direct recommendation to control this epidemic or any other specific epidemic. We make a lot of assumptions about parameters. We try to make it close to the reality, but the data has been changing every week. Instead, we suggest seeing our work as one small step into the direction of using agent-based model on temporal networks for the mentioned above problem.

2. Epidemic model and parameters. We introduce the epidemic model, which consists of three parts: population model, epidemic process and isolation. Also, we explain the choice of parameters.

2.1. *Population model.* A population is presented as a graph, where nodes are the individuals and edges correspond to the contacts between them of such a type that a considered disease can be transferred. Barabasi — Albert structure of this graph is one of the assumptions of this paper. In order to keep the narrative simple, we don't consider other types of graphs here. However, our code in [14] can be easily changed to Erdos — Reni or any other known type of graphs, and everyone is welcome to do it.
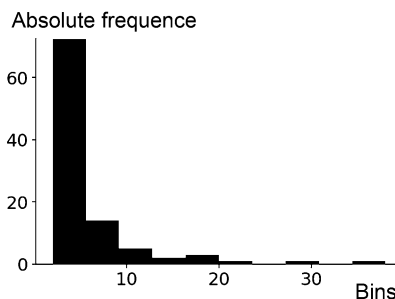

Fig. 1. Histogram of the distribution of node degrees in Barabasi graph, $n = 100$, $m = 3$

Barabasi — Albert graph of size n is built by a consecutive augmenting process [12]. After initiation of the graph G with m_0 nodes and no edges, one connects a new node x to G with $m \leqslant m_0$ edges in such a way that the probability that x is connected to $a \in G$ is equal to the degree of a. So, "popular" nodes grow faster (Fig. 1). In this work $m = m_0 = 3$.

The building process stops when the size of G reaches n. We transform G to a temporal graph by assigning the times of availability to the edges (see an example in Figures 2 and 3). Edges connect the nodes only in the assigned days of availability.
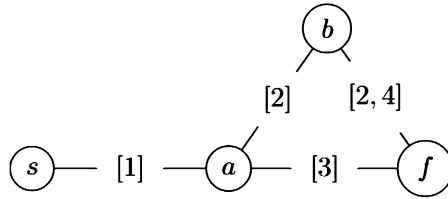

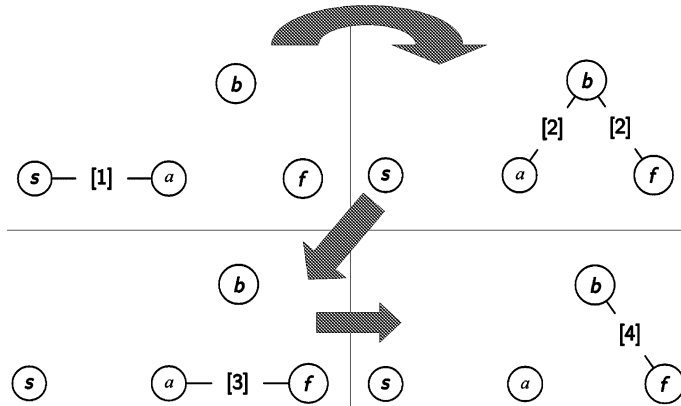*Fig. 2.* Example of a temporal graph

Fig. 3. Corresponding time sequence of static graphs for the

For instance, nodes s and a are connected by the edge (s, a) at the time 1, the nodes b and f are connected by the edge (b, f) at times 2 and 4. We assume time to be discrete, measured in days by natural numbers.

If two nodes $x, y \in G$ are connected by an edge with the assigned day of availability t, we say x and y are *temporal neighbors* at t. The number of temporal neighbors of a node $x \in G$ at t is called *temporal degree* of x at t. In Subsection 2.3 (Isolation) we will describe how we assign availability moments to the edges of the graph.

2.2. Epidemic process. When the Barabasi — Albert graph of n nodes is built we can simulate an epidemic with the SIR process (Fig. 4). If an infectious node at a day t has an available edge to a susceptible node a, then a gets infected with probability p. After 13 days a becomes recovered.

Fig. 4. Transition between the states of a node in SIR process

All recovered assumed to be immune to secondary infection during the considered epidemic. Each node in G has a status: "susceptible", "infected" or "recovered". Nodes are

infectious if and only if they have the status "infected". It may be asked why we don't have a status "dead". Despite how cruel it sounds, for the spread of the disease, dead and recovered play the same role because they can't get infected no more. After G is initiated with i infected nodes at the day zero (Figures 5, 6), every day each infectious node infects with denoted by p probability each of its temporal neighbors with the status "susceptible", meaning changing the temporal neighbor's status to "infected". The duration of status "infected" is 13 days, i. e. average duration of the infectious conditions [15, 16] after which the node becomes "recovered" (Figures 7, 8). What should the value of parameter p be? The triple product of an average temporal degree, duration of "infected" status and p should be equal to the *reproductive number* of the infection, i. e. how many new people on average get infected from one infectious. The reproductive number of COVID-19 is an open question. Different statistical methods give quite different results [17]. Here we assume that COVID-19 has reproductive number 3.6. The average temporal degree of 5000-node Barabasi-Graph is about 5.99. So, we set $p = 0.046 \approx 3.6/(5.99 \cdot 13)$. Again, these parameters should not be seen as a statement. They are just assumptions. Our goal is to present the approach rather than an actual solution. Everyone is welcome to change p and other parameters in the code at [14].
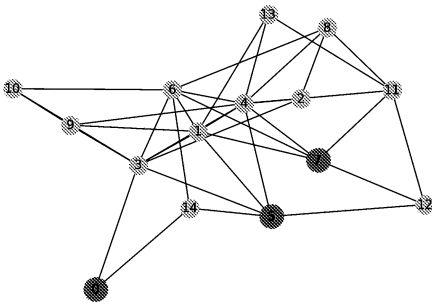

Fig. 5. Barabasi 15-node graph
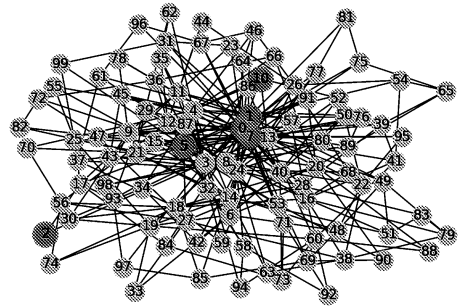with 3 infected nodes

Fig. 6. Barabasi 100-node graph
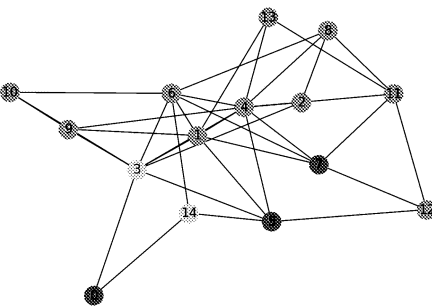with 6 initially infected

Fig. 7. Infected 15-node graph
after 15 days (blue nodes
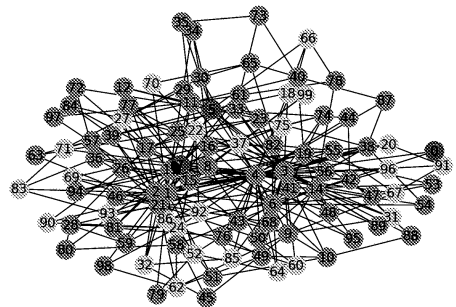represent recovered or dead)

Fig. 8. Barabasi 100-node graph
after 15 days (blue nodes
represent recovered or dead)

Since the random number generator is involved, the infection process may go differently even on the same graph and same initially infected nodes. We will address this issue in Section 3.

2.3. Isolation. One inconvenience of classic epidemic models based on differential equations or Brownian motion is that it is hard to conduct experiments with isolation. Temporal graphs allow us to do it relatively easy. First, for simplicity, we give one availability time moment per day to each edge of G during $[t_1, t_T]$, meaning that an individual maintains each of their contact daily. (In the future works, someone can try to model more complex distributions of schedules on the graph, for example, make some edges available on weekdays and others only on the weekends.) Then we enforce "No gathering 5 or more people" rule from day t_s to day t_f as following: every node $x \in G$ in the time interval $[t_s, t_f] \subset [t_1, t_T]$ disconnects from its neighbor which has temporal degree 5 or more. Since we do it in an iterative manner for all nodes in G on each time step, at some point "popular" nodes stop being "popular" and keep just few connections. The time of the beginning of isolation t_s we call *isolation delay*. Why do we choose "No gathering 5 or more people"? State of Kansas, USA, issued "Stay at Home" order [18] prohibiting mass gathering more than 10 people. However, since all the places people could gather were closed, in fact, no gatherings were happening at all. So, we assume that average number of contacts per day was less than 5 for one person.

Someone could say that isolating "popular" nodes isn't the same that "no gathering". Well, we think it is equivalent because gathering in a group of k people at day t means that the temporal degree of each person in this group greater or equal k. You may see a university lecture as a gathering of k students or you may say that their professor has a temporal degree k or higher. If students don't come in their lecture because of the "no gathering", they lower their temporal degree and the temporal degree of the professor.

3. Quality criteria. Epidemics bring complex damage to society. Individuals going through the illness work less and, in severe cases, may die. So, it makes sense to consider measures against the infection and study the effectiveness of them.

Let Ω be the space of events, causing randomness of epidemic processes.

Let $\varphi(t, t_s, l, \omega)$, further referred as *hectic function*, be the number of currently infected at a day t of the epidemic with the delay of isolation t_s, the length of isolation l and random event $\omega \in \Omega$.

As we mentioned before, the infection processes we run have random nature. Thus, to be able to make conclusions, we shall talk about expectation and variation. So, we will repeat each experiment multiple times and compute the average and standard deviation. The value $\mathrm{E}[\varphi(t, t_s, l, \omega)]$ will be estimated as $f(t, t_s, l)$, the average hectic function in the finite number of experiments.

Let $F_{\mathrm{tot}}^l(t_s)$ be the total number of people getting sick during the epidemic, i. e. $F_{\mathrm{tot}}^l(t_s) = \sum_{t=1}^{t_{\mathrm{end}}} f(t, t_s, l)/d_s$. Here t_{end} is the last day of the epidemic and d_s is duration of the infectious status. In all numerical experiments of this paper we adopt $d_s = 13$.

We choose minimality of $F_{\mathrm{tot}}^l(t_s)$ to be the first quality criterion of the actions against the epidemic.

Now let's think about lethal cases. Their number depends on the total number of infected but also depends on the available spots in hospitals. If too many ill people in severe conditions simultaneously come for medical service, there may not be enough resources to help them. Thus, another approach would be to minimize the maximum number of infected during the epidemic period (so-called "flattening"). So, the second quality criterion to be minimized is $F_{\mathrm{max}}^l(t_s) = \max_t f(t, t_s, l)$.

We consider isolation as a single tool to reduce both $F_{\mathrm{tot}}^l(t_s)$ and $F_{\mathrm{max}}^l(t_s)$. The isolation has two parameters to control: its duration l and the starting time of it t_s. The cost of isolation does depend on l. This dependency is not studied in this work, where we

make experiments with a few fixed values of l. So, we place l to the upper indices of both quality criteria and when it is fixed we name them objective functions.

In the majority of cases, the cost of isolation does not depend on t_s. This allows to perform optimization of F_{tot}^l and $F_{\max}^l$ over t_s ignoring the cost of the isolation for a fixed l.

Problem 1. Minimize the objective function

$$F_{\text{tot}}^l(t_s) = \sum_{t=1}^{t_{\text{end}}} f(t, t_s, l)/d_s = \sum_{t=1}^{t_{\text{end}}} \mathrm{E}[\varphi(t, t_s, l, \omega)]/d_s.$$

Problem 2. Minimize the objective function

$$F_{\max}^l(t_s) = \max_t f(t, t_s, l) = \max_t \mathrm{E}[\varphi(t, t_s, l, \omega)].$$

The experiments conducted in the Section 4 are meant to address the two problems above but, of course, may give some other food for thought.

4. Experiments and observations. We conducted experiments on 5000-node temporal Barabasi — Albert graph with no isolation and with the isolation of lengths $l = 14, 21$ and 42 days with delays $7, 8, ..., 14$ days. However, for simplicity of narrative, here we provide plots only for experiments with the delays $t = 7, 14$ and t_s^*. The later is the one which gives a minimal value for $F_{\max}^l$.

Each simulation is, in fact, a random process and so, we run it multiple times with non-fixed random seed. We average 30 repetitions of each simulation with corresponding l and t_s. This supplies us with estimates $\tilde{f}$ of hectic function f. Thus, we obtain estimates $\tilde{F}_{\text{tot}}^l(t_s)$ and $\tilde{F}_{\max}^l(t_s)$ of objective functions $F_{\text{tot}}^l(t_s)$ and $F_{\max}^l(t_s)$.

Estimates $\tilde{F}_{\text{tot}}^l(t_s)$ for $l = 14, 21, 42$ (2, 3, 6 weeks) and delays $t_s = 7, 8, ..., 15, \infty$, where ∞ means "No isolation", are shown in Table 1. Table 2 contains estimates $\tilde{F}_{\max}^l(t_s)$. In Tables 1 and 2 the isolation duration ℓ is in weeks, its delay t_s is in days.

Table 1. **Estimated expectations of total numbers of infected $\tilde{F}_{\text{tot}}^l$**

Delay ℓ	7	8	9	10	11	12	13	14	15	∞
2	4299	4259	4189	4131	4061	4033	3991	**3972**	3987	4453
3	4278	4189	4121	4019	3952	3879	3839	**3831**	3856	4453
6	4110	4011	3823	3653	3522	**3425**	3427	3518	3644	4453

Table 2. **Estimated expectations of maximum numbers of infected $\tilde{F}_{\max}^l$**

Delay ℓ	7	8	9	10	11	12	13	14	15	∞
2	2428	2227	1933	1645	**1540**	1714	2025	2215	2431	3217
3	2286	1895	1632	**1259**	1481	1785	1996	2219	2442	3217
6	1605	1264	**982**	1270	1492	1749	2006	2212	2399	3217

Observe that the minimum of $\tilde{F}_{\text{tot}}^l(t_s)$ have been obtained on a 14$^{\text{th}}$ day delay for 2-, 3-isolation and on 12$^{\text{th}}$ day delay for 6-week isolation. The minimum of $\tilde{F}_{\max}^l(t_s)$ has been obtained with delay equal 11, 10 and 9 for 2-, 3- and 6-week isolation, respectively.

On Figures 9 and 10 one can see the graphics of $\tilde{F}_{\text{tot}}^{14}(t_s)$ and $\tilde{F}_{\max}^{14}(t_s)$ for t_s running from 1 to 20.

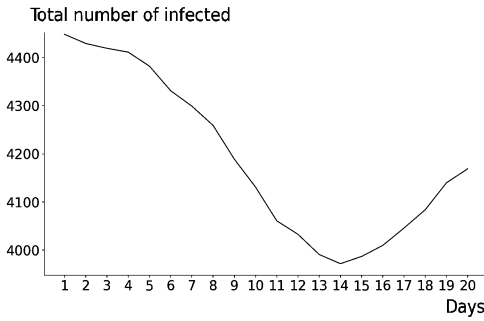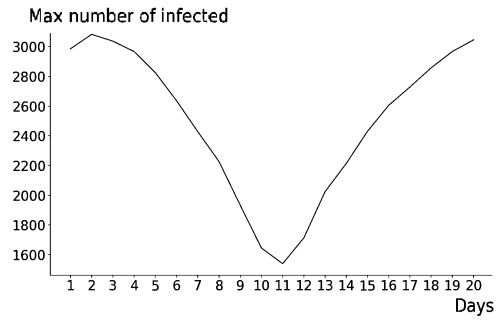Fig. 9. Values of $\widetilde{F}_{\text{tot}}^{14}$ for isolation delays from 1 to 20

Fig. 10. Values of $\widetilde{F}_{\max}^{14}$ for isolation delays from 1 to 20

Consideration of f, the expected hectic function, as a function of time with parameters l и t_s in the experiments brings us to the following observation. With big values of t_s, the function f has a single local maximum ("first wave"). With sufficiently small t_s, the second local maximum ("second wave") appears in a later time of epidemic. With the further decrease of t_s, the magnitude of the second wave is growing monotonically, meanwhile, the magnitude of the first wave is getting smaller monotonically as well (Figures 11 and 12). At some point ($t_s < 12$ for $l = 14$, $t_s < 11$ for $l = 21$,...), the first wave exceeds the second one.
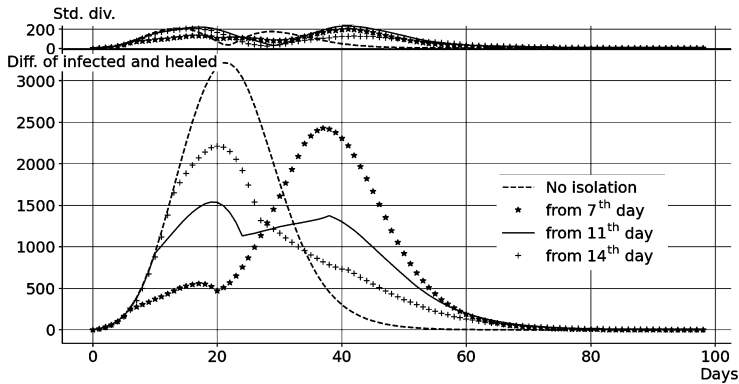

Fig. 11. Estimated hectic function on 2-week isolation with its standard deviation on the top narrow plot

One obvious conclusion from that: When the time is discretized by 1-day step, there exists a pair of delays $(\hat{t}_s, \hat{t}_s + 1)$, such that, for $\hat{t}_s$, the second wave is greater than the first wave, and otherwise for $\hat{t}_s + 1$. We have found such pairs for different l experimentally. As anticipated it appears that the maximum magnitude of both waves is minimum for one of those delays from the pair than for any other possible delay. For the convenience of comparison, the graphs of simulations for the same length of isolation are combined in one plot. Thus, we obtained three plots in Figures 11 and 12 for $l = 14, 21, 42$, respectively.

On 10 000-node graph, the results are similar. For 6-week isolation, one may see the values of the objective functions in Table 3 and the estimated hectic function with its standard deviation on the Fig. 13.
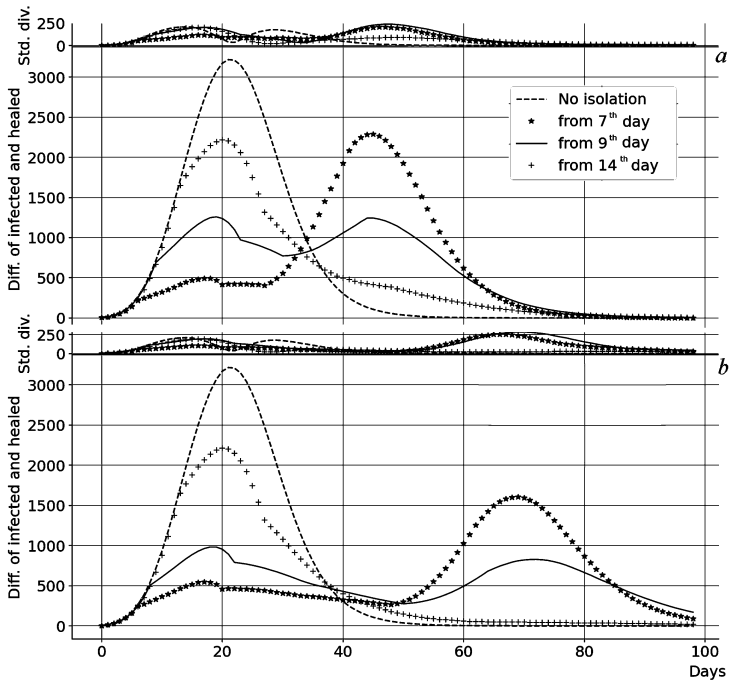
Fig. 12. Top pair *a*: estimated hectic function for 3-week isolation with its std. div. and Bottom pair *b*: estimated hectic function on 6-week isolation with its std. div.

Table 3. **Objective functions F_{tot}^{42} and $F_{\max}^{42}$ on 10K-node graph, delay in days**

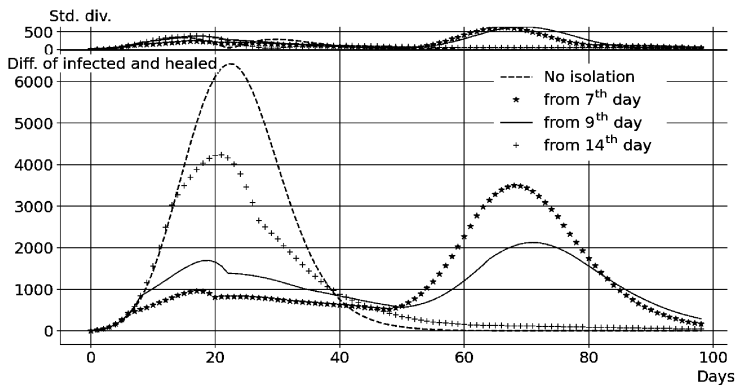| Delay / F	7	8	9	10	11	12	13	14	15	∞
F_{tot}^{42}	8306	8187	7869	7488	7211	6979	**6871**	6958	7208	8908
$F_{\max}^{42}$	3490	3019	**2126**	2197	2659	3244	3698	4229	4645	6426

Fig. 13. 10K-nodes, estimated hectic function for 6-week isolation and std. div.

In 10K-population just like in the 5K-population case, 6-week isolation brings in big sensitivity of the objective function $F_{\max}^{42}$ for the isolation delay approaching the optimal

point (9 days). Its values increases by 42 % (29 % for 5K-population) with the delay decrease by just one day. The decrease of the delay by two days causes the 64 % (63 % for 5K-population) increase of $F_{\max}^{42}$.

If one doesn't notice the scale on y-axis of Fig. 12, *b* and Fig. 13, they may think that these are the same pictures. Indeed, they are very similar. That shows that the results are well-scalable on 10K-population and, perhaps, on even bigger populations. Unfortunately, limited computer power did not let us to experiment with more than 10K-nodes.

5. SIRS. Several cases of people being infected second time several months after they recovered from COVID-19 were widely announced in the news. However, up to this moment, there is no study of the length of the obtained immunity for COVID-19. Here we suggest to look how the described above isolation experiments would look if we assume exponential decay of the immunity: $I = 2^{-t/C}$, where t is the number of days since recovery and C, the *half-life period*, is the parameter as said before we don't really know yet. Then each recovered node contacting an infectious node in the graph will be infected with probability $(1 - I)p$ instead of being forever protected like it was in SIR model. We set C to be 365 (a year) and $548 = 365 + 183$ (a year and half). That means the immunity is $2^{-1} = 0.5$ in a year or a year and a half, respectively.

With the described above modification, we have obtained the results, which are shown on Figures 14–19.
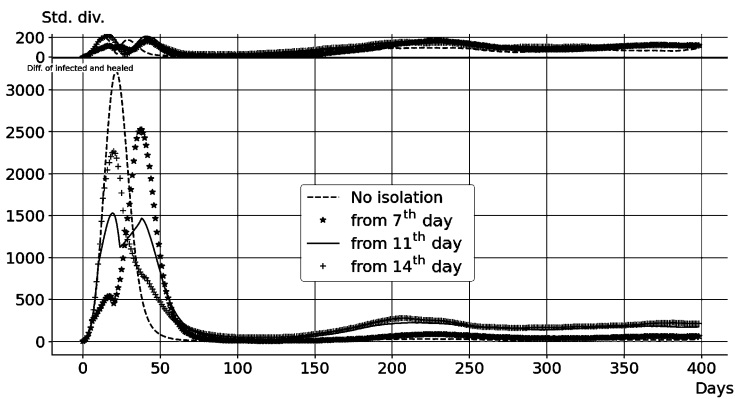

Fig. 14. 5K-nodes, estimated hectic function on 2-week isolation, half-life period $C = 365$

The first conclusion from conducted numerical experiments about the epidemic with the infection, which does not cause stable 100 % immunity for recovered is quite expected. If we compare the beginning dynamics of the epidemics with 100 % immunity and without, we will see that they coincide totally until the appearance of the first recovered. And then, with a big enough half-life period C, the dynamics are very similar to each other until the end of the last wave (if second wave doesn't exist, the first one is the last).

Thus, the beginnings of graphics in Fig. 19, in fact, are the quadruple horizontally compressed graphics in Figures 12 and 13. Similar observation can be done about graphics of mean values of hectic functions in Figures 11 and 14, 15. The same compression transforms the graphics with the delays 7, 14 days and "No isolation" in the Fig. 12 (top) to the beginnings of the graphics with the same delays in Figures 16 and 17.

Boundedness by time of immunity gives infection a chance for a long life in a population. For the convenience of the following narrative, we need to split the presence of infection in population into 3 time intervals: a) *epidemic*, rapid growth and decrease of
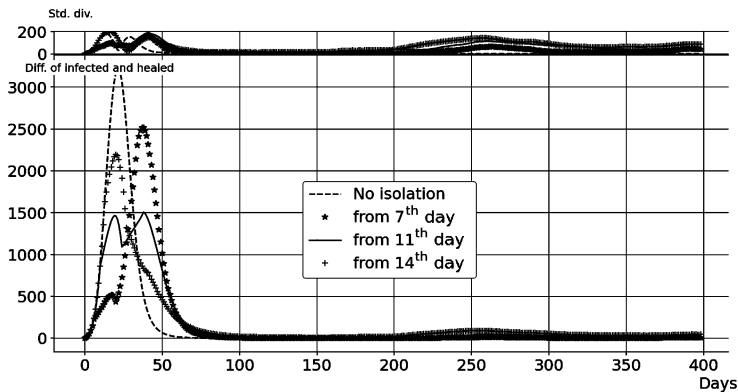
Fig. 15. 5K-nodes, estimated hectic function on 2-week isolation, half-life period $C = 548$
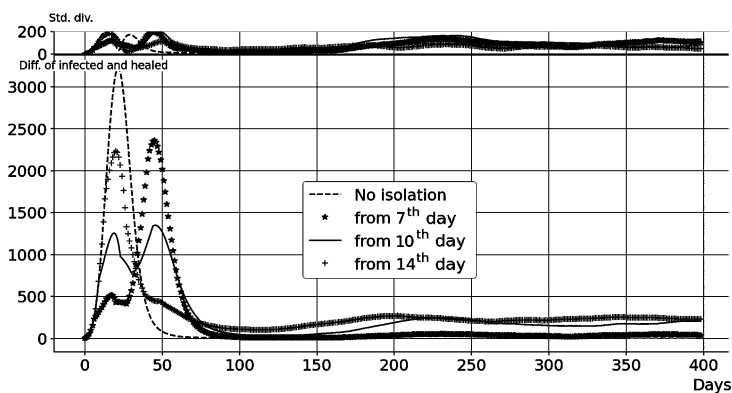

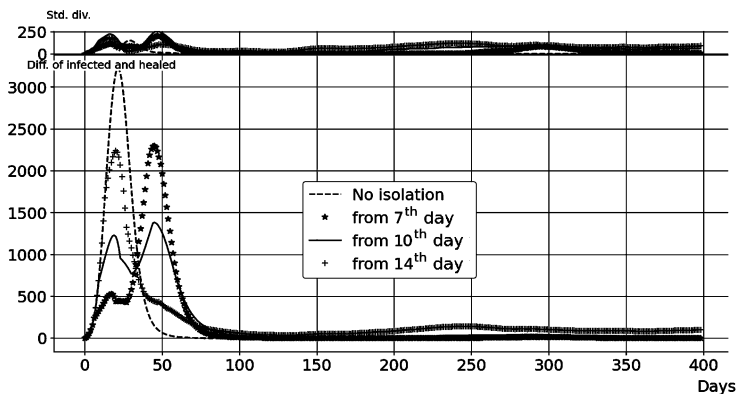*Fig. 16.* 5K-nodes, estimated hectic function on 3-week isolation, half-life period $C = 365$

Fig. 17. 5K-nodes, estimated hectic function on 3-week isolation, half-life period $C = 548$

infected (waves); b) *depression phase*, the time interval with very low number of infected, follows epidemic and has about the same length; c) *steady state*, time interval with small waves, follows depression. Obviously, these intervals don't have strict borders. Sick indi-
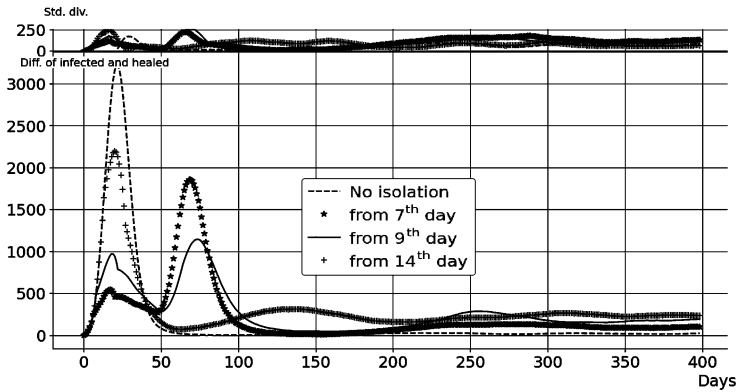
Fig. 18. 5K-nodes, estimated hectic function on 6-week isolation, half-life period $C = 365$
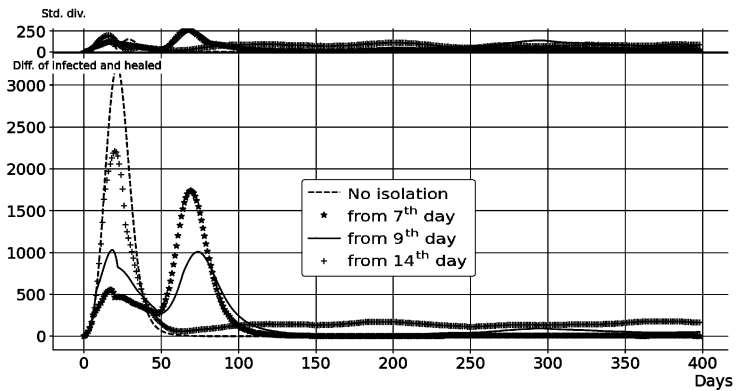

Fig. 19. 5K-nodes, estimated hectic function on 6-week isolation, half-life period $C = 548$

viduals in epidemic are first-time-infected mostly. Most of the infected of depression phase and steady state are second-timers.

We observe that the greater the magnitude of the last epidemic wave, the higher the probability that infection disappears in depression phase.

Let's demonstrate the behavior of hectic function in depression phase and steady state on the example of "No isolation" experiment on 5 000-population with half-life period $C = 365$.

So, we run 30 random processes. In all of them, we observe a single wave with almost the same magnitude, which exceeds the magnitudes of the waves in the experiments with isolation. However, in the depression phase and steady state, the numbers of infected are much lower with no isolation than with any significant (affecting the epidemic) isolation. The end of epidemic lands approximately on 60th day. At 101st day, the infection disappears in 20 processes (2/3). In the processes with the still present infection, the numbers of infected are 47, 24, 20, 16, 3, 3, 3, 2, 1, 1. Later last 7 processes nulled quickly: on 109th day — 10th process, on 114th day — 5th, one 115th day — 6th, on 119th day — 8th, on 121st day — 7th, on 129th day — 9th, on 142nd day — 4th. The remaining three processes stay alive till 400th day demonstrating chaotic oscillations with magnitude from 2 to 7 % approximately.

In the experiments with 2-week isolation delayed by 7 days, with half-life $C = 365$ the number of nulled processes at 101st day had been significantly smaller (5 from 30). Later, in depression phase lasting 106 days, this number has grown up to 23. At steady state beginning at 207th day and observed till 1095th day, oscillations of hectic function lay between 2 and 8 %.

It appears that if we assume the half-life period to be greater than a year then there is a chance that the infection continues to oppress the population.

Then with some oscillations, the estimated hectic function of survived infections has its values around 5–8 % from the population in steady phase. If we assume that C is greater than a year and a half, then, in any case, there is a day when the infection disappear from the population. Note that the last observation was obtained on relatively small populations (5000–10 000). It may not be true for larger populations.

6. Conclusion and recommendations. The experiments we conducted for SIR show that the objectives to decrease total number of infected and to decrease maximum number of infected (Problems 1 and 2 stated in Section 3) are not antagonistic to each other. Firstly, the values of both criteria improve when the delay increases starting from zero. Secondly, they get worse when the delay becomes significantly large. Thirdly, a good compromise can be found because the optimal values are achieved at closely spaced delays. For the isolation with length from 2 to 4 weeks, that compromise is the delay between 7 and 14 days.

The experiments with SIRS show that short half-life period of immunity leads to possible existence of infection in the endemic state for a long time. Then the changes of the number of infected have a wavy behavior with magnitude significantly less (around 5–8 % from the population) than in the epidemic (from 20 to 70 % depending on the isolation measures).

In some realizations of the random epidemic process with long enough half-life period C (1.5 year and more), the infection disappears after the epidemic. The share of such realizations and their magnitudes depend on C and the isolation measures. It appears that the chance that the infection leaves the population is higher when the last epidemic wave has greater magnitude.

Alas, to compute the recommendation when to start an isolation at a certain day of epidemic, besides the optimal delay t_{opt}, we need to know the day of the beginning of epidemic, which is usually unknown. Fortunately, we know n, the size of population. Also, I, the amount of infected at the current day t_{today} can be estimated. Thus, we can run "No isolation" simulation on n-node graph to the day t_1, when the number of infected in the simulation is equal to I. Then $t_{\text{today}} - t_1 + t_{\text{opt}}$ is the time to start the isolation.

References

1. Stevens H. Why outbreaks like coronavirus spread exponentially, and how to "flatten the curve". *The Washington Post*, March 14, 2020. Available at: https://www.washingtonpost.com/graphics/2020/world/corona-simulator/ (accessed: November 15, 2020).

2. Van der Hofstad R., Janssen A. J. E. M., van Leeuwaarden J. S. H. Critical epidemics, random graphs and Brownian motion with a parabolic drift. *Advances in Applied Probability*. Cambridge, Cambridge University Press, 2010, pp. 1187–1206.

3. Smith D., Moore L. The SIR model for spread of disease — the differential equation model. *MAA Publications*, Mathematical Association of America Publ., 2004. Available at: https://www.maa.org/press/periodicals/loci/joma/the-sir-model-for-spread-of-disease-the-differential-equation-model (accessed: November 15, 2020).

4. Kato F., Tainaka K., Sone S., Morita S., Iida H., Yoshimura J. Combined effects of prevention and quarantine on a breakout in SIR model. *Scientific Reports*, 2011, vol. 1, iss. 10, pp. 1–5.

5. Bo H., Yimin Z., Yongbin G., Guohui Z., Juan Z., Jin L., Li L. The analysis of isolation measures for epidemic control of COVID-19. *Applied Intelligence*, 2021, vol. 51, pp. 3074–3085.

6. Sokolov S. V., Sokolova A. L. HIV incidence in Russia: SIR epidemic model-based analysis. *Vestnik of Saint Petersburg University. Applied Mathematics. Computer Sciences. Control Processes*, 2019, vol. 15, iss. 4, pp. 616–623. https://doi.org/10.21638/11701/spbu10.2019.416

7. Zakharov V. V., Balykina Yu. E., Balansovaya model' epidemii COVID-19 na osnove procentnogo prirosta [Balance model of the COVID-19 epidemic based on percentage growth]. *Informatika i avtomatizaciya* [*Informatics and Automation*], 2021, vol. 20(5), pp. 1034–1064. https://doi.org/10.15622/20.5.2 (In Russian)

8. Sahneh F. D., Scoglio C. Epidemic spread in human networks. *2011 50th IEEE Conference on Decision and Control and European Control Conference*. Orlando, Florida, USA, 2011, pp. 3008–3013.

9. Youssef M., Scoglio C. An individual-based approach to SIR epidemics in contact networks. *J. of Theoretical Biology*, 2011, vol. 283, pp. 136–144.

10. Pereira T., Young L. Control of epidemics on complex networks: Effectiveness of delayed isolation. *Phys. Rev. E*, 2015, vol. 92, iss. 2, pp. 022822(4).

11. Alvarez-Zuzek L. G., Stanley H. E., Braunstein L. A. Epidemic model with isolation in multilayer networks. *Sci. Rep.*, 2015, vol. 5. https://doi.org/10.1038/srep12151

12. Albert R., Barabási A. Statistical mechanics of complex networks. *Rev. Mod. Phys.*, 2002, vol. 74, iss. 1, pp. 47–97.

13. Holme P., Saramäki J. Temporal networks. *Physics Reports*, 2012, vol. 519, pp. 97–125.

14. Mikheev V. IsolationSIRonBarabasi. *GitHub repository*, GitHub, 2021. Available at: https://github.com/keshmish/IsolationSIRonBarabasi.git (accessed: November 15, 2020).

15. Backer J., Klinkenberg D., Wallinga J. Incubation period of 2019 novel coronavirus (2019–nCoV) infections among travellers from Wuhan, China, January 20–28, 2020. *Euro Surveill*, 2020, vol. 25, iss. 5, no. 2000062. https://doi.org/10.2807/1560-7917.ES.2020.25.5.2000062

16. Woelfel R., Corman V., Guggemos W. Clinical presentation and virological assessment of hospitalized cases of coronavirus disease 2019 in a travel-associated transmission cluster. *medRxiv*, 2020, no. 20030502. https://doi.org/10.1101/2020.03.05.20030502

17. Liu Y., Gayle A. A., Wilder-Smith A., Rocklov J. The reproductive number of COVID-19 is higher compared to SARS coronavirus. *J. of Travel Medicine*, 2020, vol. 27, no. 2. https://doi.org/10.1093/jtm/taaa021

18. Kelly L. *Kansas Governor Stay at home order N 20-18*. Manhattan, Kansas State Government Publ., 2020. Available at: https://governor.kansas.gov/wp-content/uploads/2020/04/20-18-Executed.pdf (accessed: November 15, 2020).

A u t h o r s ' i n f o r m a t i o n :

Sergey E. Miheev — Dr. Sci. in Physics and Mathematics, Associate Professor; him2@mail.ru

Vikenty S. Mikheev — PhD in Physics and Mathematics; vikentym@ksu.edu

Критерии качества для управления эпидемическими процессами

С. Е. Михеев[1], *В. С. Михеев*[2]

[1] Санкт-Петербургский государственный университет, Российская Федерация, 199034, Санкт-Петербург, Университетская наб., 7–9

[2] Канзасский государственный университет, США, KS 66506, Манхэттен, авеню Мартина Лютера Кинга, 1228

Общее количество инфицированных до конца эпидемии и максимальное их число рассматриваются как два критерия качества для контроля эпидемиями типов SIR и SIRS посредством задержки введения изоляции. Временной граф Барабаси — Альберта используется для моделирования контактов между индивидуумами. Проведены численные эксперименты для оценки оптимальных, согласно данным критериям, задержек.

Ключевые слова: задержка введения изоляции, SIR, SIRS, управление эпидемией, временной граф Барабаси—Альберта, общее число инфицированных, максимальное число инфицированных, временная сеть.

К о н т а к т н а я   и н ф о р м а ц и я :

Михеев Сергей Евгеньевич — д-р физ.-мат. наук, доц.; him2@mail.ru

Михеев Викентий Сергеевич — канд. физ.-мат. наук; vikentym@ksu.edu